Hindawi
Journal of Engineering
Volume 2017, Article ID 2845309, 8 pages
https://doi.org/10.1155/2017/2845309

Research Article

Photoluminescence Enhancement Effect of the Layered MoS_2 Film Grown by CVD

H. Li,[1,2] X. H. Zhang,[1] and Z. K. Tang[2]

[1]*Department of Electrical and Electronic Engineering, Southern University of Science and Technology, Shenzhen 518055, China*
[2]*Institute of Applied Physics and Materials Engineering, University of Macau, Macau*

Correspondence should be addressed to X. H. Zhang; zhangxh@sustc.edu.cn and Z. K. Tang; zktang@umac.mo

Received 7 March 2017; Accepted 15 May 2017; Published 7 June 2017

Academic Editor: Qudong Wang

The layered MoS_2 films have been prepared by the chemical vapor deposition (CVD) method, which shows numerous MoS_2 convex flakes (i.e., MoS_2 nanosheets) on SiO_2/Si substrates. The convex flake islands form a uniform layered film and the single flake corresponds to one small piece of monolayer MoS_2 film; they show a strong photoluminescence (PL) radiation as a whole. The thickness of the layered MoS_2 films increases with the increases of growth time, the effect of diverse growth time on the properties of layered MoS_2 films has been discussed, and the PL enhancement effect is due to the PL intensity accumulation from each of the convex flakes. The strong PL radiation has been found by annealing the samples and the reason has been analyzed. The layered MoS_2 films could provide more photon energy than both the monolayer MoS_2 film and the bulk MoS_2. This work provides a fundamental study about the device fabrication based on layered MoS_2 films. The optoelectronic devices based on this study will be more energy efficient.

1. Introduction

Recently, transition metal dichalcogenides (TMDs), MX_2 (M = Mo, W; X = S, Se, and Te) have attracted extensive attention for their great potential in the fields of catalyst [1–4], nanoelectronic, and optoelectronic devices [2–15]. The transistors fabricated with the molybdenum disulfide (MoS_2) films demonstrate good on/off current ratio and high carrier mobility [7–10, 16–19], which make them very suitable for next generation transistors devices. Substantial works have been devoted to prepare MoS_2 films [10, 20], including mechanical exfoliation [21], liquid exfoliation [22, 23], physical vapor deposition (PVD), and CVD [2, 3, 11, 12]. However, synthesis of large-size MoS_2 single crystal films is still challenging. The thin MoS_2 film prepared by the mechanical exfoliation method based on scotch-tape can control the thickness, but the output is very low which makes it not suitable for electronic applications. The liquid exfoliation can generate large quantities of monolayer dispersions, but relatively small flakes limit their use in electronics or photonics applications. The approach of PVD is hard to achieve because of the high sublimation temperature (1100°C) and low oxidizing temperature of MoS_2. Compared with other methods, CVD is one of the most effective strategies for synthesizing large-area, high quality MoS_2 films [18, 19]. It was employed in a broad range of applications, such as FETs, LEDs, energy storage devices, and sensors, and MoS_2-based logic circuits have great potential for commercial applications in the future.

It is well known that, in bulk MoS_2, the energy band is 1.29 eV, while, in monolayer MoS_2 film, the energy band is 1.85 eV. Due to the change of band gap from bulk MoS_2 to monolayer MoS_2 film, the PL radiation appears. This phenomenon has been reported a lot [24–26], but the obvious PL radiation appeared in the layered MoS_2 films composed of convex flakes, and the strong PL radiation produced during the annealing process has not been reported before. In this work, the layered MoS_2 films is composed of many small convex flakes and exhibits relative uniformity film as a whole, so it shows a multilayer MoS_2 Raman characteristic and a monolayer MoS_2 PL characteristic simultaneously. In the layered MoS_2 films, the PL enhancement effects were observed and the reasons were analyzed.

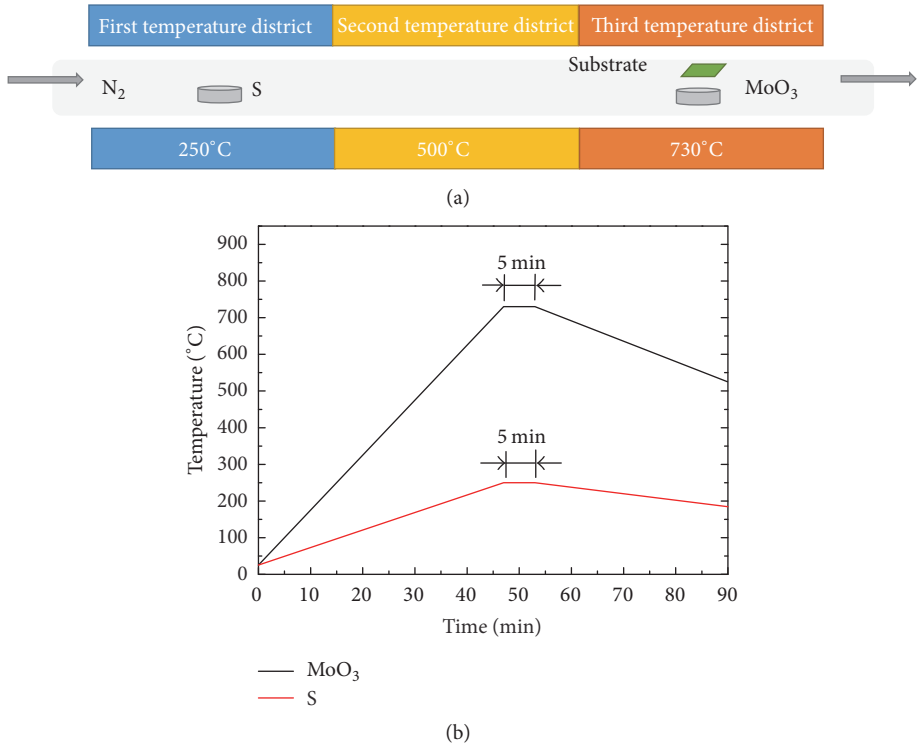

Figure 1: (a) A schematic of CVD setup for MoS_2 film growth. (b) Temperature variation curves for MoO_3 and S. MoO_3 and S with different heating rate to ensure MoO_3 and S sublimation at the same time. The 5 min growth time is labeled on the curves.

2. Experiments and Results

The MoS_2 films were grown with MoO_3 (99.95%, Sigma-Aldrich) and S (99.98%, Sigma-Aldrich) powders as precursors. MoO_3 and S powders were put in different temperature districts separately due to their different sublimation temperatures. The amount ratio between MoO_3 and S was 1 : 10, in which MoO_3 was 0.01 g and S was the 0.1 g, and the sulfur powder is completely overdosed. The size of the SiO_2/Si substrate was 10 mm × 10 mm with 300 nm thickness of SiO_2 on Si. The substrate was upside down above MoO_3 and N_2 was used as the protection gas. The N_2 flow velocity was 50 sccm mainly decided by the diameter of the quartz tube. Figure 1(a) shows a schematic of CVD setup for MoS_2 films growth. The furnace includes three temperature districts. S powder was put in the first temperature district near the N_2 entrance port and MoO_3 powder was put in the third temperature district near the N_2 exit port. The second temperature district was as a temperature transition zone. The S powder, the second temperature district, and the MoO_3 powder were raised up to 250°C, 500°C, and 730°C in 47 min, respectively, and kept at the temperature for 5 min, which aims to make sure the two precursors can be sublimation and start reaction at the same time. Then the furnace cooled down to room temperature naturally. Figure 1(b) shows the temperature variation curves for both precursors which illustrates a whole growing process of MoS_2 films by CVD method, and the growth time (chemical reaction time) of MoS_2 is 5 min. The 730°C growth temperature is the relatively low temperature for MoO_3 sublimation [27, 28], which aims to ensure the film does not grow to be too thick. The growth time is chemical reaction time of MoO_3 and S which plays a very important role for the synthesizing MoS_2 films. The layered MoS_2 films with diverse growth time (5, 10, 15, and 20 min, resp.) are synthesized, and diverse growth time leads to different growth results which will be discussed in Figure 1.

In order to observe the morphology of layered MoS_2 films, the Scanning Electron Microscope (SEM) images with diverse growth time have been shown in Figure 2. In Figure 2(a), the layered MoS_2 films were generated with 5 min growth time, a lot of convex flakes can be seen on the surface of the substrate, and they resemble standing vertically on the substrate. It should be noted that the film is actually composed of these loosed convex flakes and they form a relatively uniform film structure. Every piece convex flake corresponds to a monolayer film, and a number of convex flakes lead to strong PL radiation together. Figures 2(b) and 2(c) show the SEM images of the layered MoS_2 films with 10 and 15 min growth time, respectively. It is obvious to see the number of convex flakes less than the number generated in 5 min growth time; in 15 min growth time, the number of convex flakes is the least. It means most convex flakes accumulated into a thick film and deposited on the substrate led to the film becoming denser. Accompanied by thickening of the film, the PL intensity becomes weaker, which will be shown in Figure 2.

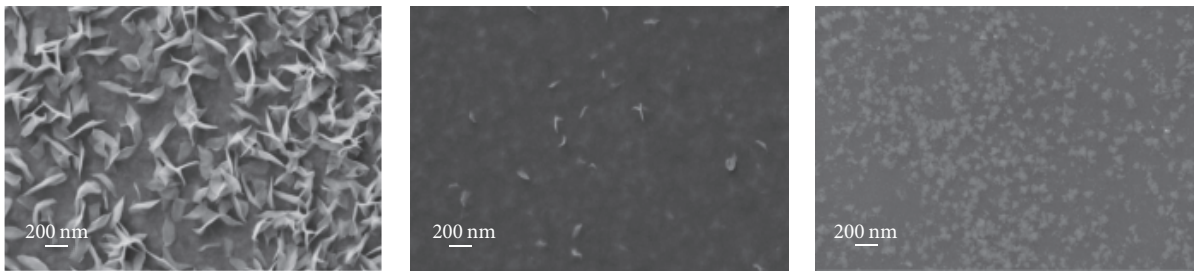

FIGURE 2: SEM images of morphology of layered MoS_2 films with (a) 5 min, (b) 10 min, and (c) 15 min growth time, respectively.

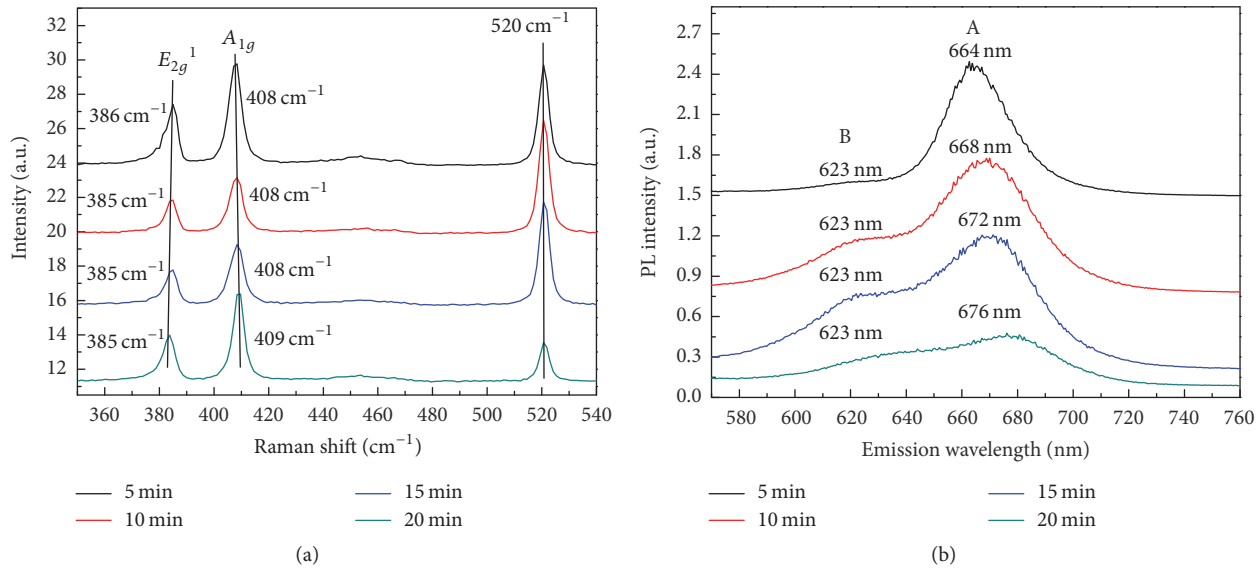

FIGURE 3: (a) Raman and (b) normalized PL spectra of layered MoS_2 films synthesized with diverse growth time. The samples are excited under 532 nm laser.

3. Analysis and Discussion

3.1. MoS_2 Synthesized with Diverse Growth Time. The Raman and PL spectra of layered MoS_2 films with diverse growth time have been measured and shown in Figures 3(a) and 3(b), respectively. There are two first-order Raman active modes (the in-of-plane vibration mode E_{2g}^1 and the out-of-plane vibration mode A_{1g}) that can be observed in Raman spectra, they are corresponding to the phonon modes of Raman scattering, and, more importantly, the two Raman active modes E_{2g}^1 and A_{1g} are regularly varied with the thicknesses of thin MoS_2 film, so they are usually used to characterize the thickness of the layered MoS_2 film [2–4, 9–11]. Take the layered MoS_2 film with growth time of 5 minutes as an example, two Raman characteristic peaks of MoS_2 are located at 386 cm^{-1} and 408 cm^{-1} (Figure 3(a)), and the difference between the two peaks ($\Delta = A_{1g\ \text{Ram shift}} - E_{2g\ \text{Ram shift}}^1$) is 22 cm^{-1}, indicating 2~3 layers' MoS_2 films according to the previous study [24–27, 29–31]. The peak at 520 cm^{-1} is the characteristic peak of Si from SiO_2/Si substrate.

The layered MoS_2 films with 10 min growth time has two characteristic peaks at 385 cm^{-1} and 408 cm^{-1}, the value of Δ is 23 cm^{-1}, according to 3~4 layers' MoS_2 films, and the result is the same as the layered MoS_2 films with 15 min growth time. When the growth time increased to 20 min, the two characteristic peaks of the layered MoS_2 films are at 385 cm^{-1} and 408 cm^{-1}, Δ equal to 24 cm^{-1}, according 4~5 layers' MoS_2 films. When the growth time increased, the frequency of the E_{2g}^1 mode decreases (red shift) and that of A_{1g} increases (blue shift), the value of Δ is increased, and the number of layers increased. It is due to the fact that restoring force between interlayer S-S bonds in layered MoS_2 is enhanced, resulting in an increase in frequency of A_{1g} mode, while the in-of-plane vibration is weakened, resulting in a red shift of the E_{2g}^1 mode. When the growth time of MoS_2 increased, the intensity of Si peak at 520 cm^{-1} reduced, also indirectly certified the thickness of the layered MoS_2 films is increased.

In order to further prove the thickness of the samples, the Atomic Force Microscope (AFM) images of MoS_2 synthesized with diverse growth time are shown in Figure 4. Due

to the convex flake structure, only the thickness of the thin sheets is investigated. Take Figure 4(a) as an example, the thickness of the film shown in the right figure is measured along the blue line in the left picture. Then the thickness is read by the height difference in the right figure. It just gives a relative thickness for fixed position, but it is still able to give an intuitive expression of the sample thickness. As we can see in Figure 4, with the extension of growth time, the film thickness increases, consistent with the results of Raman and PL spectra, and the number of layers is also consistent with results derived from the Raman spectra.

Bulk MoS_2 is one kind of indirect bandgap material and the monolayer MoS_2 is a direct bandgap material [32, 33]; it is a salient feature of MoS_2. Bulk MoS_2 shows negligible PL intensity, while monolayer MoS_2 film exhibits the strongest PL intensity. It is due to the fact that when the indirect band gap changes to the direct band gap, monolayer MoS_2 film leads to increment of radiation photon energy compared with the bulk MoS_2, which means the quantum efficiency enhances and the PL radiation increases. So the PL intensity is inversely dependent on the thickness of MoS_2 nanosheets. Normalized PL spectra of layered MoS_2 films with diverse growth time has been shown in Figure 3(b), take the sample of 5 min growth time as an example, it has two emission wavelengths at 664 nm (A exciton) and 623 nm (B exciton) [28–31], respectively, arising from the direct excitonic transitions at the Brillouin zone K point, and the energy difference between these two peaks arises from the spin-orbital splitting of the valence band. According to previous researches, only monolayer or two layers' MoS_2 film can emit the PL radiation [17, 34–36]. However, through the preparation method described above, the multilayer MoS_2 films still show a strong PL radiation (characterized by Raman spectra showed above). It is due to the fact that convex flakes structure contributes to the PL radiation accumulation, resulting in the PL enhancement effect. Every convex flake is approximate to one monolayer MoS_2 film, a lot of convex flakes stacking on the substrate approximate to many monolayer MoS_2 films, and they radiate PL together from the same small area on the substrate excited by 532 nm laser, leading to PL radiation enhancement. So the layered MoS_2 films prepared by this way have a higher MoS_2 content and provide a large number of monolayer MoS_2 nanosheets simultaneously.

When the growth time is increased, the PL intensity decreased, which means the thickness of the layered MoS_2 films increased. What is more, the peak wavelength shifts to red with the increasing of growth time (664 nm at 5 min, 668 nm at 10 min, 672 nm at 15 min, and 676 nm at 20 min). When the thickness of layered MoS_2 films increased, the layered MoS_2 films changed from direct bandgap to indirect bandgap gradually, the energy band gap decreased, so the wavelength had a red shift. The thickness of the layered MoS_2 films increased with the growth time, which is consistent with Raman spectra. That is to say, when the growth time becomes longer, more MoS_2 nanosheets are deposited on the substrate, the space among the convex flakes becomes smaller, the film becomes denser, and the PL radiation weakened. Different positions of the MoS_2 domain were measured and similar results were obtained, indicating the continuity and stability of samples.

3.2. MoS_2 Synthesized with Different Annealing Temperatures. Annealing process usually played a very important role in material preparation [19]. So the layered MoS_2 films synthesized with different annealing temperatures have also been studied. The annealing temperature changed from 780°C to 840°C with 20°C temperature spaces, respectively, and MoS_2 film without annealing was also measured for a comparison. The Raman spectra of layered MoS_2 films at different annealing temperatures are shown in Figure 5(a). Without annealing, the difference of two Raman characteristic peaks is 21 cm^{-1}, corresponding to the two atom layers. When the sample is annealed, the difference between the two Raman peaks increases as the annealing temperature increases, which means that the film becomes thicker. But the PL radiation does not become weaker correspondingly. The PL spectra are shown in Figure 5(b), and the PL intensity of annealing samples is much larger than the sample without annealing. At the beginning, with the increasing of the annealing temperature, the PL intensity increases and reaches the maximum value at 800°C, it has a great improvement compared with the MoS_2 film without annealing. Then the PL intensity decreases with the further increasing of annealing temperature, but it is still higher than the PL intensity of MoS_2 film without annealing. A stronger PL enhancement effect has been shown in the annealing samples because more defeats were induced to the samples and more convex flakes were generated on the substrates. The layered MoS_2 film has the strongest PL radiation at 800°C, the optimal annealing temperature means the best temperature for the convex flakes generation.

In order to further understand the mechanism behind the different growth conditions, the X-ray diffraction (XRD) spectra are measured for both samples with diverse growth time and different annealing temperatures. As we can see in Figure 6(a), with the increase in growth time, more crystal orientations appear, and the intensity of (002) peak increases, and the results proved that the samples transform from layered MoS_2 to bulk MoS_2, resulting in an enlargement of the difference value between the two Raman characteristic peaks, consistent with the Raman spectra shown in Figure 5(a), which means the film becomes thicker. In Figure 6(b), after the samples have been annealed, the (100) peak disappears and the (102) peak appears, and different crystalline orientations may cause the change in the PL intensity. When the annealing temperature increases, the full width at half maximum (FWHM) of (002) peak increases, indicating that the grain size becomes smaller. The intensity of (002) peak is proportional to degree of bulk material [37]. At 800°C annealing temperature, the intensity of (002) peak is weakest, and the PL intensity is strongest, which shows the highest degree for film formation, which is consistent with the PL spectra in Figure 5(b). More importantly, PL intensity of layered MoS_2 is proportional to defect density and impurity concentration [38]. The introduction of more defects in the annealing process is also one reason for PL radiation enhancement.

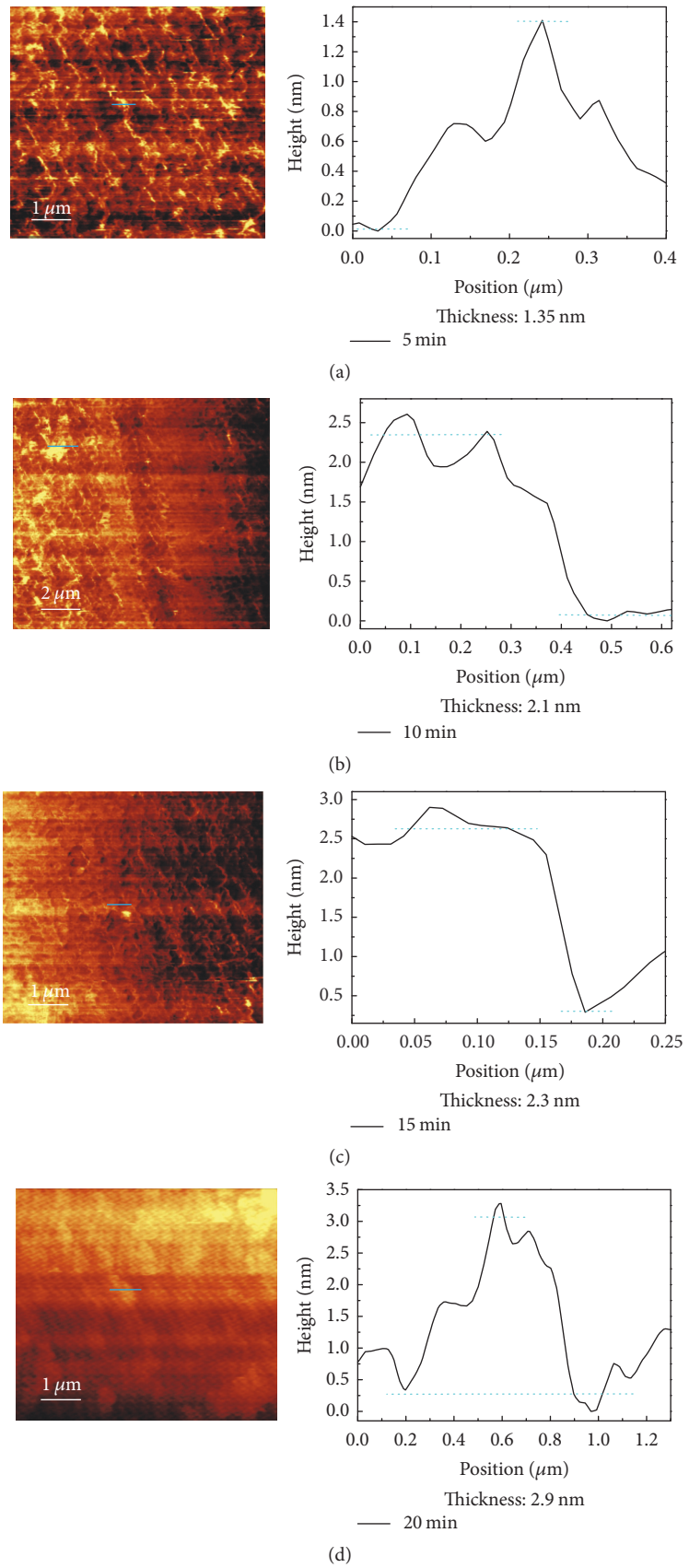

Figure 4: AFM images of MoS_2 synthesized with (a) 5 min, (b) 10 min, (c) 15 min, and (d) 20 min growth time.

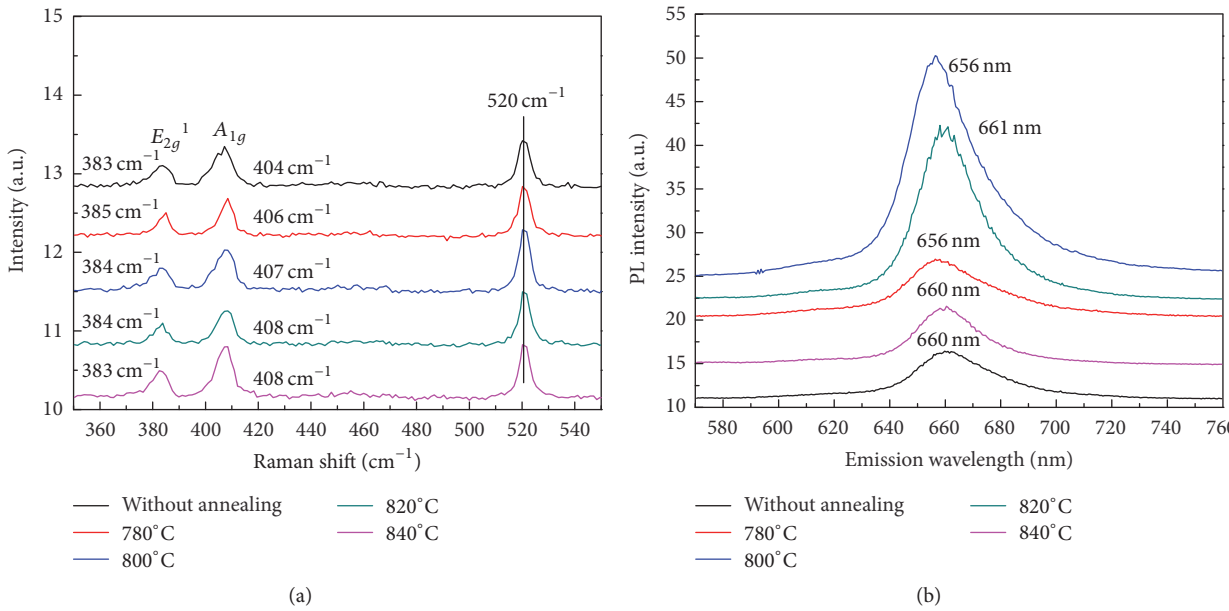

FIGURE 5: (a) Raman and (b) PL spectra of layered MoS_2 film synthesized at different annealing temperatures. The annealing temperature changed from 780°C to 840°C with 20°C temperature spaces, respectively. The MoS_2 film synthesized without annealing is also shown as a comparison. All measurements were carried out at the same experiment conditions.

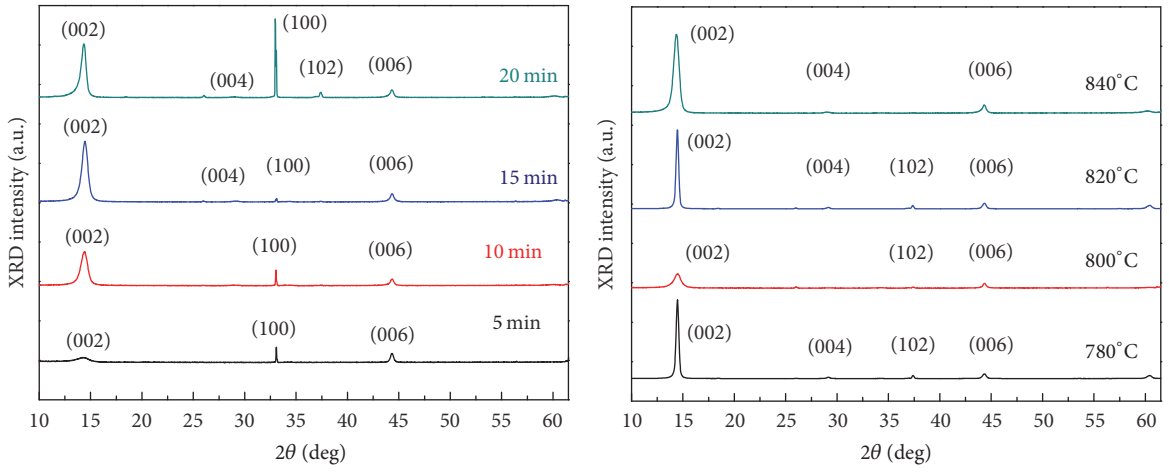

FIGURE 6: XRD spectrum of MoS_2 synthesized with (a) diverse growth time and (b) different annealing temperatures.

4. Conclusions

In this paper, the layered MoS_2 films on SiO_2/Si substrates have been prepared by CVD method. It is composed of lots of MoS_2 convex flakes, each convex flake corresponding to a monolayer MoS_2 film which has a PL radiation, and lots of convex flakes showed strong PL radiation as a whole. The effect of diverse growth time on the quality of the layered MoS_2 films has been discussed, and the strongest PL radiation has been observed on the layered MoS_2 films with 5 min growth time. A strong PL enhancement effect was found after the samples were annealed, and the strongest PL intensity has been obtained under the growth condition of 730°C and annealing at 800°C. It provides a foundation study for preparation of layered MoS_2 film by CVD. In the previous study, it usually could not observe so strong PL radiation when the difference between the two characteristic Raman peaks exceeded 20 cm^{-1}, but, due to the MoS_2 convex flakes structure, the monolayer and multilayer MoS_2 films coexist on the substrate, and the samples have a higher MoS_2 content and provided a monolayer component simultaneously. So it could provide more charge carriers and 2D component when it is used in optoelectronics devices. This work provides a new choice about the device fabrication based on the layered MoS_2 films generated by CVD method. It could provide more photon energy due to more charge carriers

that emerged through the direct band transition. The optoelectronic devices based on this study will be more energy efficient and environmentally friendly and are of interest to the development of sustainable energy.

Conflicts of Interest

The authors declare that there are no conflicts of interest regarding the publication of this paper.

Acknowledgments

The authors would like to acknowledge the support of Natural Science Foundation of Guangdong Province under Grant no. 2014A030313728.

References

[1] Y. Li, H. Wang, L. Xie, Y. Liang, G. Hong, and H. Dai, "MoS_2 nanoparticles grown on graphene: an advanced catalyst for the hydrogen evolution reaction," *Journal of the American Chemical Society*, vol. 133, no. 19, pp. 7296–7299, 2011.

[2] S. Balendhran, S. Walia, H. Nili et al., "Two-dimensional molybdenum trioxide and dichalcogenides," *Advanced Functional Materials*, vol. 23, no. 32, pp. 3952–3970, 2013.

[3] R. Ganatra and Q. Zhang, "Few-layer MoS_2: a promising layered semiconductor," *ACS Nano*, vol. 8, no. 5, pp. 4074–4099, 2014.

[4] S. Wang, Y. Rong, Y. Fan et al., "Shape evolution of monolayer MoS_2 crystals grown by chemical vapor deposition," *Chemistry of Materials*, vol. 26, no. 22, pp. 6371–6379, 2014.

[5] Y.-H. Chang, W. Zhang, Y. Zhu et al., "Monolayer $MoSe_2$ grown by chemical vapor deposition for fast photodetection," *ACS Nano*, vol. 8, no. 8, pp. 8582–8590, 2014.

[6] S. Wu, C. Huang, G. Aivazian, J. S. Ross, D. H. Cobden, and X. Xu, "Vapor-solid growth of high optical quality MoS_2 monolayers with near-unity valley polarization," *ACS Nano*, vol. 7, no. 3, pp. 2768–2772, 2013.

[7] M.-Y. Lin, C.-E. Chang, C.-H. Wang et al., "Toward epitaxially grown two-dimensional crystal hetero-structures: single and double MoS_2/graphene hetero-structures by chemical vapor depositions," *Applied Physics Letters*, vol. 105, no. 7, Article ID 073501, 2014.

[8] D. J. Late, B. Liu, H. S. S. R. Matte, V. P. Dravid, and C. N. R. Rao, "Hysteresis in single-layer MoS_2 field effect transistors," *ACS Nano*, vol. 6, no. 6, pp. 5635–5641, 2012.

[9] Y.-H. Lee, X.-Q. Zhang, W. Zhang et al., "Synthesis of large-area MoS_2 atomic layers with chemical vapor deposition," *Advanced Materials*, vol. 24, no. 17, pp. 2320–2325, 2012.

[10] Q. H. Wang, K. Kalantar-Zadeh, A. Kis, J. N. Coleman, and M. S. Strano, "Electronics and optoelectronics of two-dimensional transition metal dichalcogenides," *Nature Nanotechnology*, vol. 7, no. 11, pp. 699–712, 2012.

[11] Y. Cao, X. Luo, S. Han et al., "Influences of carrier gas flow rate on the morphologies of MoS_2 flakes," *Chemical Physics Letters*, vol. 631-632, pp. 30–33, 2015.

[12] X. Lu, M. I. B. Utama, J. Lin et al., "Large-area synthesis of monolayer and few-layer $MoSe_2$ films on SiO_2 substrates," *Nano Letters*, vol. 14, no. 5, pp. 2419–2425, 2014.

[13] A. Gurarslan, Y. Yu, L. Su et al., "Surface-energy-assisted perfect transfer of centimeter-scale monolayer and few-layer MoS_2 films onto arbitrary substrates," *ACS Nano*, vol. 8, no. 11, pp. 11522–11528, 2014.

[14] S. H. Baek, Y. Choi, and W. Choi, "Large-area growth of uniform single-layer MoS_2 thin films by chemical vapor deposition," *Nanoscale Research Letters*, vol. 10, article 388, 2015.

[15] Y.-H. Lee, L. Yu, H. Wang et al., "Synthesis and transfer of single-layer transition metal disulfides on diverse surfaces," *Nano Letters*, vol. 13, no. 4, pp. 1852–1857, 2013.

[16] J. H. Kim, J. Lee, J. H. Kim, C. C. Hwang, C. Lee, and J. Y. Park, "Work function variation of MoS_2 atomic layers grown with chemical vapor deposition: the effects of thickness and the adsorption of water/oxygen molecules," *Applied Physics Letters*, vol. 106, Article ID 251606, 2015.

[17] K.-K. Liu, W. Zhang, Y.-H. Lee et al., "Growth of large-area and highly crystalline MoS_2 thin layers on insulating substrates," *Nano Letters*, vol. 12, no. 3, pp. 1538–1544, 2012.

[18] Y. Yu, C. Li, Y. Liu, L. Su, Y. Zhang, and L. Cao, "Controlled scalable synthesis of uniform, high-quality monolayer and few-layer MoS_2 films," *Scientific Reports*, vol. 3, article 1866, 2013.

[19] X. Wang, H. Feng, Y. Wu, and L. Jiao, "Controlled synthesis of highly crystalline MoS_2 flakes by chemical vapor deposition," *Journal of the American Chemical Society*, vol. 135, no. 14, pp. 5304–5307, 2013.

[20] M. Chhowalla, H. S. Shin, G. Eda, L.-J. Li, K. P. Loh, and H. Zhang, "The chemistry of two-dimensional layered transition metal dichalcogenide nanosheets," *Nature Chemistry*, vol. 5, no. 4, pp. 263–275, 2013.

[21] K. S. Novoselov, D. Jiang, F. Schedin et al., "Two-dimensional atomic crystals," *Proceedings of the National Academy of Sciences of the United States of America*, vol. 102, no. 30, pp. 10451–10453, 2005.

[22] J. N. Coleman, M. Lotya, A. O'Neill et al., "Two-dimensional nanosheets produced by liquid exfoliation of layered materials," *Science*, vol. 331, pp. 568–571, 2011.

[23] V. Nicolosi, M. Chhowalla, M. G. Kanatzidis, M. S. Strano, and J. N. Coleman, "Liquid exfoliation of layered materials," *Science*, vol. 340, no. 6139, Article ID 1226419, 2013.

[24] M. Xu, T. Liang, M. Shi, and H. Chen, "Graphene-like two-dimensional materials," *Chemical Reviews*, vol. 113, no. 5, pp. 3766–3798, 2013.

[25] R. Ionescu, W. Wang, Y. Chai et al., "Synthesis of atomically thin MoS_2 triangles and hexagrams and their electrical transport properties," *IEEE Transactions on Nanotechnology*, vol. 13, no. 4, pp. 749–754, 2014.

[26] A. M. Van Der Zande, P. Y. Huang, D. A. Chenet et al., "Grains and grain boundaries in highly crystalline monolayer molybdenum disulphide," *Nature Materials*, vol. 12, no. 6, pp. 554–561, 2013.

[27] S. Najmaei, Z. Liu, W. Zhou et al., "Vapour phase growth and grain boundary structure of molybdenum disulphide atomic layers," *Nature Materials*, vol. 12, no. 8, pp. 754–759, 2013.

[28] Y. Lee, S. Park, H. Kim, G. H. Han, Y. H. Lee, and J. Kim, "Characterization of the structural defects in CVD-grown monolayered MoS_2 using near-field photoluminescence imaging," *Nanoscale*, vol. 7, no. 28, pp. 11909–11914, 2015.

[29] Y. Huang, J. Guo, Y. Kang, Y. Ai, and C. M. Li, "Two dimensional atomically thin MoS_2 nanosheets and their sensing applications," *Nanoscale*, vol. 7, no. 46, pp. 19358–19376, 2015.

[30] D. Qiu, D. U. Lee, S. W. Pak, and E. K. Kim, "Structural and optical properties of MoS_2 layers grown by successive two-step chemical vapor deposition method," *Thin Solid Films*, vol. 587, pp. 47–51, 2015.

[31] D. W. Kim, J. M. Ok, W.-B. Jung et al., "Direct observation of molybdenum disulfide, MoS_2, domains by using a liquid crystalline texture method," *Nano Letters*, vol. 15, no. 1, pp. 229–234, 2015.

[32] X. Huang, Z. Zeng, and H. Zhang, "Metal dichalcogenide nanosheets: preparation, properties and applications," *Chemical Society Reviews*, vol. 42, pp. 1934–1946, 2013.

[33] M. Ye, D. Winslow, D. Zhang, R. Pandey, and Y. K. Yap, "Recent advancement on the optical properties of two-dimensional molybdenum disulfide (MoS_2) thin films," *Photonics*, vol. 2, no. 1, pp. 288–307, 2015.

[34] A. Splendiani, L. Sun, Y. Zhang et al., "Emerging photoluminescence in monolayer MoS_2," *Nano Letters*, vol. 10, no. 4, pp. 1271–1275, 2010.

[35] H. Liu and D. Chi, "Dispersive growth and laser-induced rippling of large-area singlelayer MoS_2 nanosheets by CVD on c-plane sapphire substrate," *Scientific Reports*, vol. 5, article 11756, 2015.

[36] X. Ling, Y.-H. Lee, Y. Lin et al., "Role of the seeding promoter in MoS_2 growth by chemical vapor deposition," *Nano Letters*, vol. 14, no. 2, pp. 464–472, 2014.

[37] D. Gao, M. Si, J. Li et al., "Ferromagnetism in freestanding MoS_2 nanosheets," *Nanoscale Research Letters*, vol. 8, article 129, 2013.

[38] H. Nan, Z. Wang, W. Wang et al., "Strong photoluminescence enhancement of MoS_2 through defect engineering and oxygen bonding," *ACS Nano*, vol. 8, no. 6, pp. 5738–5745, 2014.